

Thermodynamics of ionization and dissociation in hydrogen plasmas including fluctuations and magnetic fields

Werner Ebeling^a, Hendrik Hache^b, and Michael Spahn^c

Institut für Physik, Humboldt-Universität zu Berlin, Invalidenstr. 110, 10115 Berlin, Germany

14th June 2018

Abstract Applying Gibb's geometrical methods to the thermodynamics of H-plasmas we explore the landscape of the free energy as a function of the degrees of ionization and dissociation. Several approximations for the free energy are discussed. We show that in the region of partial ionization/dissociation the quantum Debye-Hückel approximation (QDHA) yields a rather good but still simple representation which allows to include magnetic field and fluctuation effects. By using relations of Onsager-Landau-type the probability of fluctuations and ionization/dissociation processes are described. We show that the degrees of ionization/dissociation are probabilistic quantities which are subject to a relatively large dispersion. Magnetic field effects are studied.

PACS. 52.25.Kn Thermodynamics of plasmas – 52.27.Gr Strongly-coupled plasmas – 05.70.Ln Nonequilibrium and irreversible thermodynamics

1 Introduction

In plasmas and in particular in hydrogen systems, ionization and dissociation processes play an important role. We find the equilibrium values of the degrees of ionization and dissociation by minimization of the free energy at fixed total mass [1, 2, 3]. Further the ionization and dissociation rates are derived from kinetic equations [2, 4]. Here we will start with a study of the geometry of the free energy landscape [5, 6]. The idea to apply geometrical methods in thermodynamical research goes back to pioneering papers of Gibbs [7]. We apply Gibb's method here to plasmas. We will study different approximations to the thermodynamic functions and the influence of several effects, our approach is limited to the region $T > 10000K$. In a preceding work we have developed a similar approach for ionization processes described by the Saha equation [6]. We include here also effects of magnetic fields which are of increasing interest not only for astrophysical applications but also for plasmas confined in magnetic traps. A preliminary work on magnetic field effects was published earlier [8]. The magnetic field introduces an anisotropy into the system. This changes the ideal gas contribution, the bound state energies and the contributions due to interactions of the free particles. Here we will take into account the ideal gas corrections in an exact way, and the bound state and interaction corrections in approximations which include

the quadratic orders in the field $O(B^2)$. Practically this restricts our approach to fields $B < 10^5 T$.

We start with exploring the geometry of the free energy landscape as a function of the degrees of ionization and dissociation. On this basis we are able to describe not only the chemical equilibria but also fluctuations around the equilibrium values [5].

2 The free energy density of hydrogen

2.1 Defining the basic variables of the system

We consider in the following hydrogen plasmas at fixed temperature T , and proton density n . Our aim is to study ionization processes



and dissociation processes



For simplicity, the formation of H_2^+ and H^- species will be neglected.

In order to define the thermodynamics of the system we introduce the free energy

$$F(T, V, \{N\}), \quad (3)$$

the density of the free energy

$$f(T, n) = \frac{F}{V} = f(T, n_e, n_i, n_a, n_m), \quad (4)$$

^a e-mail: ebeling@physik.hu-berlin.de

^b e-mail: hache@physik.hu-berlin.de

^c e-mail: spahn@physik.hu-berlin.de

the degrees of ionization and dissociation [3]. We will use here the following definitions:

$$\alpha = \frac{n_i}{n_i + n_a + 2n_m} \quad \beta = \frac{n_a}{n_a + 2n_m} \quad (5)$$

$$\beta_a = \frac{n_a}{n_i + n_a + 2n_m} \quad \beta_m = \frac{2n_m}{n_i + n_a + 2n_m}.$$

We note that β_a is the relative amount of protons bound in atoms and β_m the relative amount bound in molecules. Due to the balance relation for the total proton density

$$n = n_i + n_a + 2n_m. \quad (6)$$

we find the relations

$$\beta_a = (1 - \alpha)\beta, \quad \beta_m = (1 - \alpha)(1 - \beta). \quad (7)$$

The condition of neutrality requires that electron and ion densities are always equal:

$$n_e = n_i. \quad (8)$$

Therefore the free energy density depends only on 4 independent parameters

$$f \Rightarrow f(T, n, \alpha, \beta). \quad (9)$$

If we include magnetic field effects we have 5 independent parameters

$$f \Rightarrow f(T, n, B, \alpha, \beta). \quad (10)$$

The equilibrium composition is found by the minimization procedure

$$\frac{\delta f}{\delta \alpha} = 0, \quad \frac{\delta f}{\delta \beta} = 0. \quad (11)$$

Instead of β we may use β_a or β_m as variational parameters. The relation

$$\alpha + \beta_a + \beta_m = 1 \quad (12)$$

gives the possibility for visualization of the free energy surface on a simplex.

2.2 The different contributions to the free energy

We assume the following structure [2,3]:

$$f = f_e^{id} + f_i^{id} + f_a^{id} + f_m^{id} + f_{ee} + f_{ii} + f_{ie} + f_{hs}. \quad (13)$$

The first 3 terms describe the ideal contributions of the electrons, ions, atoms and molecules. The next 3 terms represent the Coulomb interactions electron-electron, ion-ion, and ion-electron. For these terms different approximations exist as e.g. the quantum Debye-Hückel-approximation (QDHA) and Padé approximation [1]. Basically we will use here the QDHA:

$$f_{ee} + f_{ii} + f_{ie} \approx f_{DH}. \quad (14)$$

In the QDHA screening and quantum effects are both taken into account in a first approximation. The inclusion of further effects as Hartree-Fock etc. by means of Padé approximations makes no principal difficulties but increases the numerical efforts. We will show that in the region of partial ionization and dissociation the QDHA yields a reasonable description of ionization/dissociation phenomena. The interactions of the neutral components are taken into account by hard core approximation including effects of reduced volume [2,3].

We will discuss now these contributions in more detail:

- the ideal free energy of electrons f_e^{id} . We use Fermi-Dirac statistics including excluded volume corrections representing the free energy in the following way [2]:

$$f_e = n_e k_B T \cdot z \left(\frac{1}{2} \frac{n_e \Lambda_e^3}{1 - \eta_0} \right). \quad (15)$$

The function $z(x)$ which is due to Zimmermann [2] interpolates between the low density limit: $z(x) \approx \ln x - 1$ and the high density limit: $z(x) \propto x^{\frac{2}{3}}$. Further $\Lambda_e = h/\sqrt{2\pi m_e k_B T}$ is the thermal wave length of the electrons, correspondingly we will use next the thermal wave lengths of ions, atoms and molecules (Λ_i , Λ_a , Λ_m). The excluded volume factor $\eta_0 < 1$ expresses that some part of the total volume V which is occupied by atoms and molecules is not accessible to the electrons. The accessible volume $(1 - \eta_0)V$ is smaller than the total volume and the effective densities are higher. A strict theory for η_0 is not yet available. We will use here

$$\eta_0 = \frac{4}{3} \pi R_0^3 (n_a + 2n_m) \quad (16)$$

as the definition for the packing parameter with an estimate for the atomic radius $R_0 = 0.78 \text{Å}$. Effects of a magnetic field are included by the replacement [8]

$$n_e \Lambda_e^3 \rightarrow n_e \Lambda_e^3 \frac{\tanh(x_e)}{x_e}, \quad (17)$$

where $x_e = \hbar \omega_c^e / 2k_B T$ and $\omega_c^e = eB/m_e$.

- the ideal free energy of the ions f_i^{id} which is given by the classical term

$$f_i^{id} = n_i k_B T [\ln(n_i \Lambda_i^3) - 1] - n_i k_B T \ln(1 - \eta_0). \quad (18)$$

The second term describes the excluded volume effect for the classical bare protons [2]. The parameter $x_i = \hbar \omega_c^i / 2k_B T$ ($\omega_c^i = eB/m_i$) is very small $x_i \ll 1$ for small B . Therefore the magnetic field effects can be neglected for protons.

- the ideal atom contribution: f_a^{id} . We assume Boltzmann statistics i.e.

$$f_a^{id} = n_a k_B T \left[\ln \left(\frac{n_a \Lambda_a^3}{\sigma_a} \right) - 1 \right] \quad (19)$$

including the internal states by a Brillouin-Planck-Larkin partition function [2]

$$\sigma_a(\xi) = \sum_{n=1}^{\infty} n^2 \left\{ e^{\left(\frac{\xi}{2}\right)^2 \frac{1}{n^2}} - 1 - \left(\frac{\xi}{2}\right)^2 \frac{1}{n^2} \right\}, \quad (20)$$

where $\xi = 2\sqrt{\text{Ry}/k_B T}$ with the ionization energy of hydrogen $\text{Ry} \simeq 13.598\text{eV}$. Including the magnetic field we have to replace the atomic partition function σ_a by an effective partition function,

$$\sigma_a(T) \rightarrow \sigma_{\text{eff}}(T, B), \quad (21)$$

which reads [8]

$$\sigma_{\text{eff}}(T, B) = \sigma_a(\xi_e) + \frac{x_e^2}{24} \left[\sigma_B(\xi_e) + \frac{\xi_e^4}{192} \left(1 + \frac{\pi^2}{3} \right) \right] \quad (22)$$

with the interaction parameter $\xi_e = e^2/4\pi\epsilon_0 k_B T \lambda_e$ ($\lambda_e = \hbar/\sqrt{2m_e k_B T}$ is the thermal wave length for the relative motion of electrons and protons (with an infinit proton mass)) and [8]

$$\begin{aligned} \sigma_B(\xi) = & \sum_{n=1}^{\infty} 2n^2(1+n^2) \left[e^{\left(\frac{\xi}{2}\right)^2 \frac{1}{n^2}} - 1 - \left(\frac{\xi}{2}\right)^2 \frac{1}{n^2} \right. \\ & - \frac{1}{2!} \left(\frac{\xi}{2}\right)^4 \frac{1}{n^4} \left. - \sum_{n=1}^{\infty} n^4(5+7n^2) \left(\frac{2}{\xi}\right)^2 \right. \\ & \times \left[e^{\left(\frac{\xi}{2}\right)^2 \frac{1}{n^2}} - 1 - \left(\frac{\xi}{2}\right)^2 \frac{1}{n^2} - \frac{1}{2!} \left(\frac{\xi}{2}\right)^4 \frac{1}{n^4} \right. \\ & \left. \left. + \frac{1}{3!} \left(\frac{\xi}{2}\right)^6 \frac{1}{n^6} \right] \right]. \quad (23) \end{aligned}$$

- the molecular contribution: f_m^{id} . We will use the representation [3]

$$f_m^{id} = n_m k_B T \left[\ln \left(\frac{n_m \Lambda_m^3}{\sigma_m} \right) - 1 \right] + f_m^{vib} + f_m^{rot} \quad (24)$$

including the internal molecular and atomic states,

$$\sigma_m = \sigma_a^2 \exp \left(\frac{4.746\text{eV}}{k_B T} \right), \quad (25)$$

and the contributions of vibrational and rotational states [9]

$$f_m^{vib} = n_m k_B T \left[\ln \left(1 - e^{-\frac{T_v}{T}} \right) + \frac{T_v}{2T} \right], \quad (26)$$

$$T_v = 6210\text{K}$$

$$f_m^{rot} = n_m k_B T \left[\ln \frac{T_r}{T} - \frac{T_r}{3T} - \frac{1}{90} \left(\frac{T_r}{T} \right)^2 \right], \quad (27)$$

$$T_r = 85\text{K}.$$

- the Debye-Hückel contribution f_{DH} . Using here the so-called $\frac{A}{8}$ -approximation [2] we arrive at the formula

$$f_{DH} = -k_B T \frac{\kappa^3}{12\pi} \tau(\kappa a(T)). \quad (28)$$

Here the inverse Debye-radius is defined by

$$\kappa = \sqrt{\frac{2n_i e^2}{\epsilon_0 k_B T}} \quad (29)$$

and the effective thermal electron radius by

$$a(T) = \frac{\Lambda_e}{8} \quad (30)$$

where Λ_e is the electron thermal wave length defined above. Further the τ -function has the standard Debye-Hückel form [1]:

$$\tau(x) = \frac{3}{x^3} \left[\ln(1+x) - x + \frac{x^2}{2} \right]. \quad (31)$$

The advantage of the QDHA is that magnetic field effects may easily taken into account by a factor [8]

$$a(T) \rightarrow a(T, x_e) = a(T) \cdot \left[1 - \frac{1}{48} x_e^2 \right]. \quad (32)$$

The magnetic field reduces the effective diameter. This reflects the fact that the magnetic field localizes the particles perpendicular to the field.

- the hard-core contribution f_{hs} . For this term we use the Carnahan-Starling approximation [2]:

$$f_{hs} = k_B T \frac{(n_a + 2n_m)(4\eta - 3\eta^2)}{(1 - \eta)^2}. \quad (33)$$

The volume fraction of the neutrals is here defined by the effective packing parameter

$$\eta = \frac{4\pi}{3} R^3 (n_a + 2n_m). \quad (34)$$

Following the work of Juranek and Redmer [10] we fix the effective packing radius of atoms at a mean value $R = 0.37\text{\AA}$. This is of course a rough approximation which might be refined by taking into account different radii for the atoms and for the molecules and by introducing temperature-dependent radii based on fluid variational theory [10].

3 Discussion of the approximations and influence of parameters

For this section we neglect the magnetic field, i.e. we assume $B = 0$. We are interested in partial ionization and dissociation, i.e. in the region of the density-temperature plane where electrons, ions, atoms, and molecules exist. In this region the electrons may show quantum effects but the ions, atoms, and molecules are still classical.

The excluded volume effect, i.e. the effect that the electrons and ions cannot penetrate into the neutral particles, are taken into account in the ideal contributions. The excluded volume factor η_0 is defined above with a fixed radius R_0 . If this effect is not considered we find a lower ionization rate α at higher densities, shown in figure 1.

A small difference of the radius R_0 has an influence on the degree of ionization and dissociation, see figure 1. For larger radii, α begins to increase at smaller densities

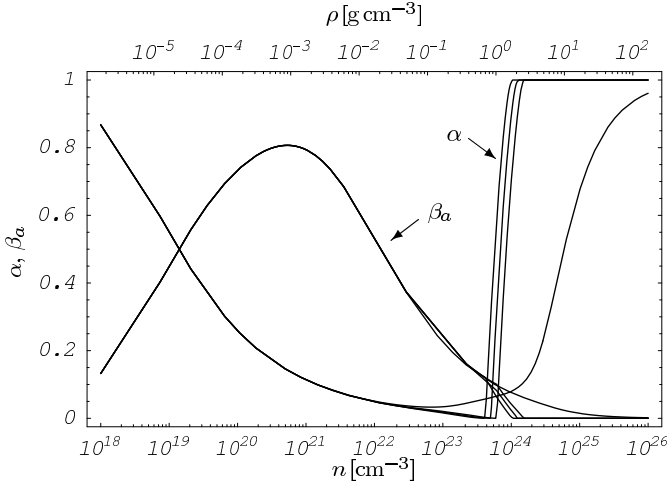


Figure 1. Degree of Ionization and dissociation for different radii R_0 at a temperature of $T = 2 \cdot 10^4$ K. From right to left: $R_0 = 0$, $R_0 = 0.73 \text{ \AA}$, $R_0 = 0.78 \text{ \AA}$, and $R_0 = 0.83 \text{ \AA}$

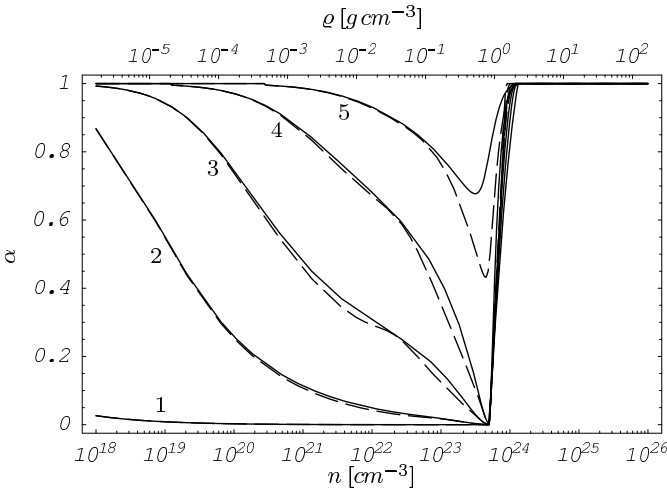


Figure 2. Degree of Ionization as a function of the total proton density for different temperatures: (1) $T = 10^4$ K, (2) $T = 2 \cdot 10^4$ K, (3) $T = 3 \cdot 10^4$ K, (4) $T = 5 \cdot 10^4$ K, (5) $T = 10^5$ K. The solid line represents the Calculation with the QDHA and the dashed line with Padé approximation.

since the effective volume $V_{\text{eff}} = (1 - \eta_0)V$, which is available for the electrons, decreases with increasing η_0 and thus increases the effective electron density $n_e^{\text{eff}} = n_e/V_{\text{eff}}$. Therefore the system tends to higher degrees of ionization. The transition between low and complete degrees of ionization takes place in a very narrow density range. For high densities the excluded volume effect has to be considered and has still to be refined maybe by taking into account temperature dependencies of the radius [10] and by introducing occupation probabilities [11, 12, 13].

The nonideal effects of the free charged particles can be described more correctly by means of Padé approximation (see e. g. [14, 15, 16]). Figure 2 shows the ionization and dissociation rate as a function of the proton density calculated by using the QDHA and by the Padé formulae given in [15]. For the density range of $10^{22} - 10^{25} \text{ cm}^{-3}$

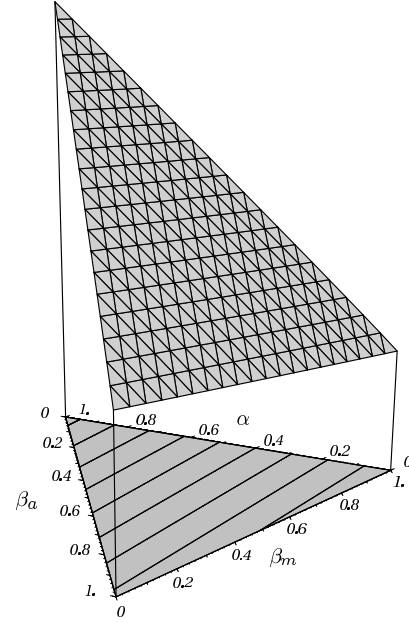


Figure 3. Free energy density at $T = 300$ K, $n = 2 \cdot 10^{19} \text{ cm}^{-3}$ represented on the simplex α, β_a, β_m . The minimum of the free energy is at the corner $\alpha = 0, \beta_a = 0, \beta_m = 1$, i.e. in equilibrium we find practically only molecules.

and the temperature range $1 \cdot 10^4 - 5 \cdot 10^4$ K we find only small deviations of the QDHA from the Padé approach. For higher temperatures above 10^5 K the deviations are much larger and the QDHA is less accurate. In the following we will restrict our study to temperatures much below 10^5 K, therefore it is justified to use further the QDHA to simplify the formulae and to reduce calculation efforts.

4 The geometry of the free energy landscape

On the basis of the formulae given in section 2 we represented the geometry with respect to $f(\alpha, \beta)$ at fixed T , n and starting with $B = 0$ (figures 3, 4). We used the variables α, β_a , and β_m which allow a representation on a simplex according to eq. (12). The minimum of the free energy corresponds to the stationary degrees of ionization and dissociation. The form of the landscape around the minimum determines the thermal fluctuations.

Depending on the values of temperature and proton density we find different locations of the minimum. At $T = 300$ K, $n = 2 \cdot 10^{19} \text{ cm}^{-3}$ we observe a minimum in the corner $\alpha = 0, \beta_a = 0, \beta_m = 1$, meaning that only molecules exist (figure 3). At different temperature and proton density, e.g. $T = 4 \cdot 10^4$ K, $n = 10^{22} \text{ cm}^{-3}$ we observe a minimum in the center of the simplex. This corresponds to a situation where free electrons and ions and bound states (atoms and molecules) exist under the same conditions (figure 4).

With the procedure described above we calculated the stationary degrees of ionization and dissociation for a lattice of points in the temperature-density-plane. In this way

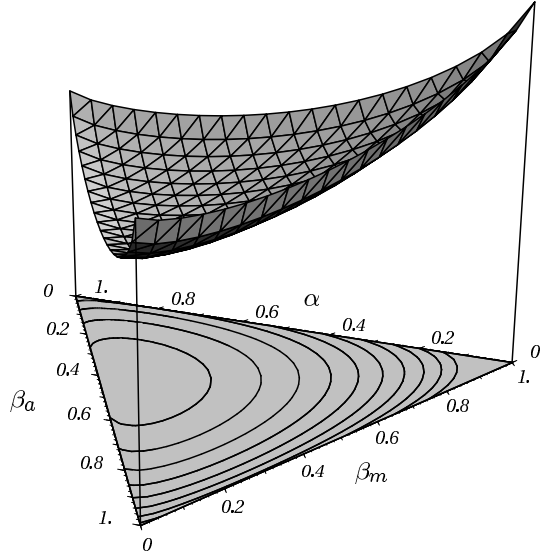


Figure 4. Free energy density at $T = 4 \cdot 10^4 \text{ K}$, $n = 10^{22} \text{ cm}^{-3}$. The minimum is found in a region where electrons, ions, atoms and molecules are present.

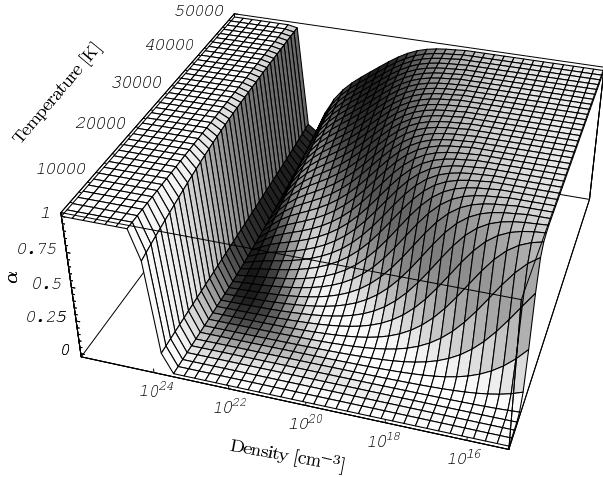


Figure 5. The degree of ionization α together with the dispersion of α as a function of the proton density and the temperature. The coding is such that light regions correspond to small dispersion and dark regions correspond to large dispersion.

we obtained the degree of ionization as a function of density and temperature (figure 5).

We observe full ionization ($\alpha = 1$ on a plateau in the upper right corner and at the left edge of the diagram) at very high densities and in the region of lower densities but high temperatures. At sufficiently low density we find only bound states when the temperature is low ($\alpha = 0$ in a region beginning at the lower edge of the diagram). In the intermediate region of proton densities we find a valley of bound states stretching over the whole temperature range with small ionization taking place only at very high temperatures [1].

Now we will look at the formation of molecules (figure 6). We observe similar features as above in the corresponding parameter regions. At very high densities (left edge)

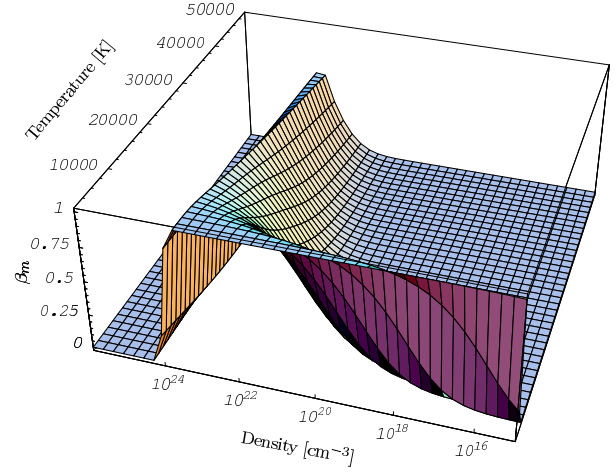


Figure 6. The fraction of protons bound in molecules $\beta_m = (1 - \alpha)(1 - \beta)$

no molecules exist as well as in the region of lower densities and high temperatures (upper right corner). When the density is sufficiently low and the temperature is low as well we find that the bound states observed in figure 5 are practically only made up of molecules ($\beta_m \approx 1$ at the lower edge). In the intermediate density region we find a mountain of molecules ($\beta_m = 1$) and a decline of the degree of dissociation with rising temperature.

5 Fluctuations according to Boltzmann-Gibbs

Let us first consider the general schema of the theory of isothermal fluctuations at given temperature T [17,18]. We follow Klimontovich who developed the general fluctuation theory of Boltzmann and Gibbs [18]. In the general case we study a set of intrinsic parameters $A(X, a) = (A_1(X, a), \dots, A_n(X, a))$ depending on dynamical variables X and external parameters a and define a conditional free energy $F(a, T|A)$ which is the free energy at fixed values $A = A(X, a)$. The intrinsic parameters $A(x, a)$ do not need to have any thermodynamic functions which correspond to them. The equilibrium value of the free energy is $F(a, T)$. Then according to the Boltzmann-Gibbs principle the probabilities of fluctuations of A are given by

$$p(A|a, T) = \exp \left[\frac{F(a, T) - F(a, T|A)}{k_B T} \right]. \quad (35)$$

In our case the dynamical variables are $A = \{\alpha, \beta\}$, for F we choose the free energy per proton $\phi = f/n$ with the equilibrium value $\phi_0 = f_0/n$ at fixed temperature T .

Then according to the Boltzmann-Gibbs principle the probability distribution of isothermal fluctuations reads

$$p(\alpha, \beta|n, T) = \frac{e^{\frac{\phi_0 - \phi(\alpha, \beta)}{k_B T}}}{\sum_{\alpha, \beta} e^{\frac{\phi_0 - \phi(\alpha, \beta)}{k_B T}}}. \quad (36)$$

An illustration of the probability distribution calculated

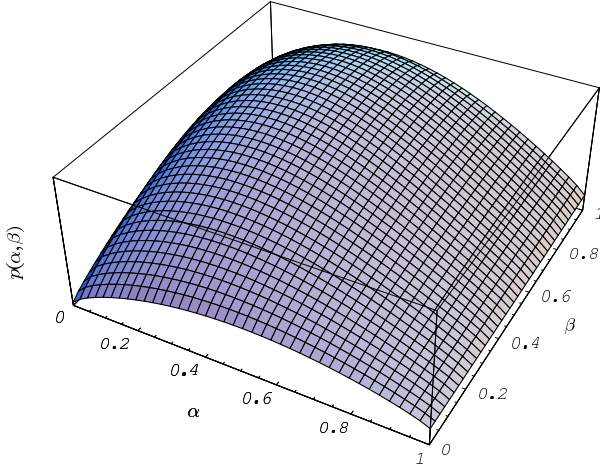


Figure 7. The probability distribution in the α, β -plane at $T = 3 \cdot 10^4 \text{ K}$ and $n = 10^{22} \text{ cm}^{-3}$

for a lattice of 50×50 points on the α, β -plane is shown in figure 7.

Further we show in figure 5 the degree of ionization together with the dispersion of the degree of ionization coded in gray levels. The diagram was obtained with the following procedure: For a given temperature and proton density the stationary degrees of ionization and dissociation $(\bar{\alpha}, \bar{\beta})$ were calculated. Then we additionally fixed the degree of dissociation at its stationary value $\beta = \bar{\beta}$ and calculated the probability $p(\alpha)$ to find arbitrary values for the degree of ionization. The dispersion of the degree of ionization $(\delta\alpha)^2 = \overline{(\alpha - \bar{\alpha})^2}$ was then calculated as the root of the mean quadratic deviation from the stationary value $\bar{\alpha}$.

We observe low dispersion (light) at very high densities due to the hard-sphere contribution. High dispersion (dark) is observed in two transition regions, one when ionization processes start taking place at intermediate densities and temperatures (just above $\alpha = 0$), the other at the transition to complete ionization (just below $\alpha = 1$) where the remaining bound states break up.

Inside the simplex we assume that the probability distribution function $p(\alpha, \beta = \bar{\beta})$ is an one dimensional gaussian distribution for values α inside the borders and for small fluctuations $\delta\alpha = \alpha - \bar{\alpha}$

$$p(\alpha) = C \exp \left[-\frac{1}{2k_B T} \left(\frac{\partial^2 \phi}{\partial \alpha^2} \right)_{\alpha=\bar{\alpha}} (\alpha - \bar{\alpha})^2 \right] \quad (37)$$

where $\bar{\alpha}$ is the equilibrium value and therefore the most probable value. The constant C is determined from the normalization. The dispersion in the fluctuations is given by

$$\overline{(\delta\alpha)^2} = k_B T \left[\left(\frac{\partial^2 \phi}{\partial \alpha^2} \right)_{\alpha=\bar{\alpha}} \right]^{-1}. \quad (38)$$

We see that the second deviation of $\phi(\alpha, \beta = \bar{\beta})$, which is the curvature of the free energy landscape determines the dispersion $\overline{(\delta\alpha)^2}$. Near to the corner of the simplex the distribution is highly non-gaussian and highly unsymmetrical. In this case the border of frequent fluctuations (the

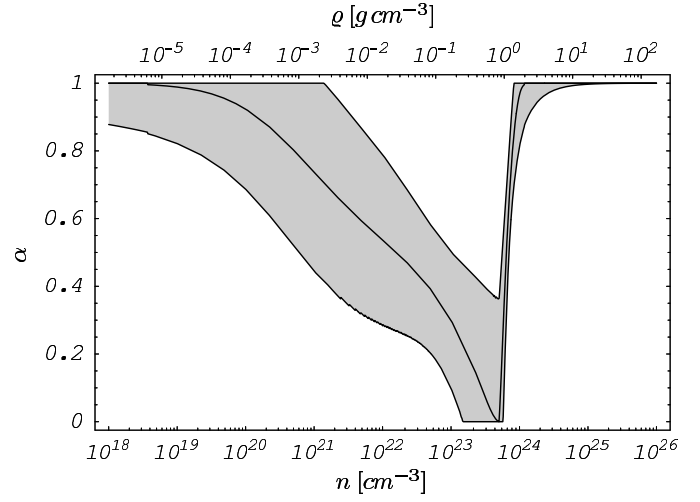


Figure 8. Degree of ionization as a function of the proton density n with the dispersion of the fluctuations of α at $T = 4 \cdot 10^4 \text{ K}$.

range of the dispersion) may be estimated by finding the roots of $p(\alpha) \simeq p(\alpha = \bar{\alpha})/\sqrt{e}$. For gaussian distributions this criterion agrees with the one given above.

In density-temperature regions where the minimum of the free energy is developed very well e.g. if the minimum is located in a corner of the simplex (see e.g. figure 3) we have small dispersions. Is the free energy landscape flat e.g. if the minimum is located inside the simplex (see e.g. figure 4) we have large dispersions.

To further illustrate this, we show the dispersion of the degree of ionization at fixed temperature, corresponding to a cut through the diagram in figure 5 parallel to the n -axis. The dispersion is indicated by error bars, which are cut at the physically impossible values $\alpha > 1$ and $\alpha < 0$ (figure 8). Again the dispersion is small at high and low densities and is high near the transition $\alpha = 1 \Rightarrow \alpha < 1$ where bound states emerge.

6 Magnetic field effects

We want to discuss now the influence of a constant uniform magnetic field on the ionization and dissociation equilibrium. We have to carry out the replacements (17), (21), and (32). These formulae equations are valid for weak magnetic fields, i.e.

$$\frac{x_e^2}{48} \ll 1. \quad (39)$$

In figure 9 the degree of ionization and dissociation for various magnetic field strengths are plotted over the temperature. We find at a fixed density that the degree of ionization of a plasma in a magnetic field is higher compared to the field free case and increases with the field strength. For temperatures higher than 10^5 K and weak magnetic fields there are no differences in the ionization degree. Further we see in figure 10 that the curves deviate in the mid-density range where atoms and molecules

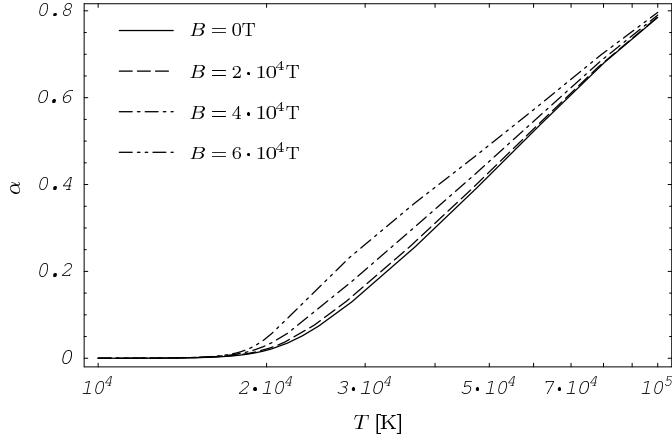


Figure 9. Degree of ionization and dissociation for different magnetic field strengths at a proton density $n = 10^{23} \text{ cm}^{-3}$.

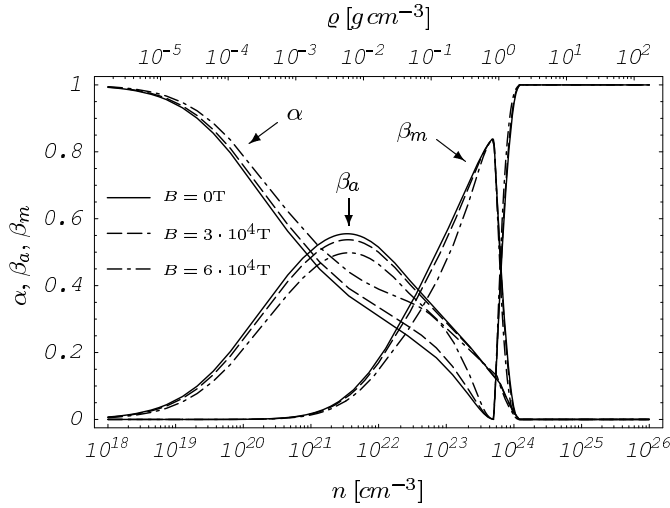


Figure 10. Degree of Ionization and dissociation for different magnetic fields at a temperature $T = 3 \cdot 10^4 \text{ K}$.

exist up to the density where the transition to complete ionization takes place.

7 Conclusions

Based on a detailed study of the free energy landscape we developed a new description of ionization and dissociation phenomena. The relatively simple approximation QDHA used for the interaction term in the free energy allows the study of the dispersion of the degrees of ionization and dissociation and of magnetic field effects. The QDHA may be replaced by more refined approximations as Padé approximation. We have shown that the study of free energy landscapes in combination with the fluctuation theory yields relevant information on dispersion of the degrees of ionization and dissociation. The natural dispersion is usually in the range of 5 – 10% except on the borders. This has consequences for many experimental quantities as e.g. conductivity and optical properties. Since the conductivity is in first approximation proportional to α , i.e. $\sigma \sim \alpha \sigma_0$, we

may conclude that the thermal dispersion of the plasma conductivity σ has nearly the same shape as the dispersion of α . We note that the thermal fluctuations of α , β , σ etc. are in general not of Gaussian character what is due to the existence of borders as e.g. $0 \leq \alpha \leq 1$. Studying the influence of magnetic fields we have shown that a remarkable influence on the degree of ionization starts at $B \sim 10^4 \text{ T}$, the effects increase with the magnetic field strength. At fields $B \gtrsim 5 \cdot 10^4 \text{ T}$ the degree of ionization and also the conductivity and other related quantities are substantially higher than for the field free case, the present approach however is no more valid at these extremely high fields.

Recent experimental work on dense hydrogen concentrates mainly on Hugoniot [19]. The approach presented here is restricted to temperatures $T > 10000 \text{ K}$, therefore it cannot be used for the calculation of the low-temperature parts of Hugoniot. An extension taking into account recent results on the low temperature EOS of dense hydrogen [2] is in progress.

The authors thank Stefan Hilbert, Hauke Juranek, Ronald Redmer, Gerd Röpke, Manfred Schlages and Werner Stolzmann for many helpful discussions. The authors W. Ebeling and H. Hache profited very much from a stay at the Rostock University.

References

1. W. Ebeling, W.D. Kraeft, and D. Kremp. *Theory of Bound States and Ionization Equilibria*. Akademie-Verlag, Berlin, 1976.
2. W. Ebeling, A. Förster, V.E. Fortov, V.K. Gryaznov, and A.Ya. Polishchuk. *Thermophysical Properties of Hot Dense Plasmas*. Teubner, Stuttgart/Leipzig, 1991.
3. D. Beule, W. Ebeling, A. Förster, H. Juranek, S. Nagel, R. Redmer, and G. Röpke. *Phys. Rev. B*, 59:14177, 1999.
4. Yu.L. Klimontovich. *Kinetic Theory of Nonideal Gases and Plasmas*. Pergamon Press, Oxford, 1982.
5. W. Ebeling. *Contr. Plasma Phys.*, 30:553–561, 1990.
6. W. Ebeling and S. Hilbert. *Eur. Phys. J. D*, 20:93–101, 2002.
7. J. W. Gibbs. *Thermodynamische Studien*. Verlag von Wilhelm Engelmann, Leipzig, 1892.
8. W. Ebeling, M. Steinberg, and J. Ortner. *Eur. Phys. J. D*, 12:513–520, 2000.
9. R. Fowler and E. A. Guggenheim. *Statistical Thermodynamics*. Cambridge University Press, Cambridge, 1952.
10. H. Juranek and R. Redmer. *J. Chem. Phys.*, 112:3780–3786, 2000.
11. D. Saumon and G. Chabrier. *Phys. Rev. A*, 44:5122–5140, 1991.
12. A. Potekhin. *Phys. Plasmas*, 3:4196, 1996.
13. G. Chabrier and A. Potekhin. *Phys. Rev. E*, 58:4941, 1998.
14. W. Ebeling and W. Richert. *Phys. Stat. Sol. (b)*, 128:467–474, 1985.
15. W. Stolzmann and W. Ebeling. *Phys. Lett. A*, 248:242–248, 1998.
16. W. Stolzmann and T. Blöcker. *Astron. Astrophys.*, 361:1152–1168, 2000.

17. L.D. Landau and E.M. Lifshitz. *Statistical Physics*. Pergamon Press, Oxford, 1958.
18. Yu.L. Klimontovich. *Statistical Theory of Open Systems*. Kluwer, Dordrecht, 1995.
19. M.D. Knudson, D.L. Hanson, J.E. Bailey, C.A. Hall, J.R. Asay, and W.W. Anderson. *Phys. Rev. Lett.*, 87:225501, 2001.